Magnetic Moment of the Positive Muon*

DAVID P. HUTCHINSON,†‡ JACK MENES,§ AND G. SHAPIRO‖
Columbia University, New York, New York

AND

A. M. PATLACH
I. B. M. Watson Laboratory, New York, New York

(Received 3 January 1963)

The magnetic moment of the positive muon has been redetermined in terms of proton moments using a precession technique. The sensitivity achieved yields an error of 13 parts per million. The muons are stopped in various targets in a homogeneous magnetic field. The anisotropic distribution of the decay electrons relative to the muon spin direction permits the measurement of the spin precession frequency. The proton spin resonance is measured in the same field, yielding $f_\mu/f_p=3.18338\pm0.00004$. This result may be combined with that of other experiments, the muon g factor, and the ratio of electron cyclotron frequency to proton resonance, f_e/f_p, to obtain a more precise evaluation of the muon mass in terms of electron masses. m_μ/m_e equals 206.765 ± 0.005.

I. INTRODUCTION

IT is well known[1] that the muon interacts with other particles as if it were a heavy electron, any differences in the observed properties of muon and electron being entirely explained by the greater mass of the muon. To measure the extent of this similarity, there have been many measurements in recent years of the fundamental properties of the muon and, where possible, comparison of these with the same electron property.

The discovery that muon decay was not parity conserving and that cyclotron muon beams were polarized[2] led to the first measurement of the muon magnetic moment.[3] The anisotropic distribution of the decay electrons relative to the muon spin direction makes possible the measurement of the precession frequency of the muon in a magnetic field. As the muon has spin equal one-half,[4,5] the precession frequency is related to the magnetic moment by

$$f=\frac{2M_H H}{2\pi\hbar},\quad M_H=g\frac{e}{2mc}\frac{\hbar}{2},$$

where f is the precession frequency; g, the g factor; e, the muon charge; m, the mass; H, the magnetic field intensity; and M_H, the maximum component of the magnetic moment in the field direction.

It is of considerable interest to measure the magnetic moment in terms of muon magnetons; i.e., to measure the g factor of the muon because of the exact prediction of this quantity made by quantum electrodynamics.[6,7] This measurement and previous measurements of the moment[3,8,9] have been made in terms of the proton magnetic moment. The g factor, calculated via the above equation, requires a knowledge of the muon mass. The best independent determinations of the muon mass have a precision of 10^{-4} which contributes most to the error in g since the moment measurement reported here has a precision of the order of 10^{-5} and the other factors necessary to the calculation of g are known even more precisely.

Recently, there has been a direct measurement of the muon g factor at CERN[10] to a precision of 10^{-5}. The result is in agreement with theory. As this exceeds by a factor of 10 our ability to measure g indirectly and there is no immediate prospect of an independent measurement of the muon mass to 10^{-5}, we may invert the procedure of past experiments by using the g factor determination of CERN in conjunction with our measurement of the muon magnetic moment to obtain a more precise evaluation of the muon mass.

II. PRECESSION METHOD OF MUON MOMENT DETERMINATION

The method used in this experiment is a refinement of methods used previously at the University of Chicago

* Work supported in part by the U. S. Office of Naval Research.
† Submitted in partial fulfillment of the requirements for the degree of Doctor of Philosophy in the Faculty of Pure Science, Columbia University.
‡ Present address: University of Pennsylvania, Philadelphia, Pennsylvania.
§ Present address: Brookhaven National Laboratory, Upton, New York.
‖ Present address: Lawrence Radiation Laboratory, Berkeley, California.
[1] For example, M. Gell-Mann, Rev. Mod. Phys. **31**, 834 (1959).
[2] R. L. Garwin, L. M. Lederman, and M. Weinrich, Phys. Rev. **105**, 1415 (1957).
[3] T. Coffin, R. L. Garwin, S. Penman, L. M. Lederman, and A. M. Sachs, Phys. Rev. **109**, 973 (1958).
[4] W. Frati and J. Rainwater, Phys. Rev. **128**, 2360 (1962).
[5] V. Hughes, D. McColm, K. Ziock, and R. Prepost, Phys. Rev. Letters **5**, 63 (1960).
[6] H. Suura and E. H. Wichman, Phys. Rev. **105**, 1930 (1957).
[7] A. Petermann, Phys. Rev. **105**, 1931 (1957).
[8] R. A. Lundy, J. C. Sens, R. A. Swanson, V. L. Telegdi, and D. D. Yovanovich, Phys. Rev. Letters **1**, 38 (1958).
[9] R. L. Garwin, D. P. Hutchinson, S. Penman, and G. Shapiro, Phys. Rev. **118**, 271 (1960). See also, G. Shapiro, thesis [Nevis Report No. 79 (unpublished)].
[10] G. Charpak, F. J. M. Farley, R. L. Garwin, T. Muller, J. C. Sens, V. L. Telegdi, and A. Zichichi, Phys. Rev. Letters **6**, 128 (1961); G. Charpak, F. J. M. Farley, R. L. Garwin, T. Muller, J. C. Sens, and A. Zichichi, *A New Measurement of the Anomalous Magnetic Moment of the Muon* (CERN, Geneva, Switzerland, 1962).

and at Columbia University.[8,9] This is described completely in Ref. 9, but will be outlined here for the reader's convenience.

A longitudinally polarized beam of positive muons is stopped in a vertical magnetic field. Their spin precesses about the field direction until they decay into electrons (e^+) and neutrinos. Due to the correlation of decay probability with spin direction, the counting rate for decay electrons in a fixed direction varies with time according to

$$N_e(t)=e^{-t/\tau}[1+a\cos(\omega_H t-\theta_0)],$$

where τ is the muon lifetime, 2.2 μsec, ω_H' the spin precession frequency, a, the asymmetry coefficient, and θ_0 is a constant determined by the initial polarization of the muon.

The first factor in $N_e(t)$ is due to the muon lifetime, the second to its anisotropic decay.

The time difference, t, between muon stopping and decay is measured by means of a continuously running reference oscillator of angular frequency ω_0. It is not necessary to know the integral number of cycles of the reference oscillator in time t. Only the phase angle, ϕ, in excess of the integral number of cycles is recorded. Thus, ϕ ranges from 0 to 2π. Since ω_0 is made almost equal to ω_H, ϕ is almost equal to $\omega_H t$ (but for an arbitrary constant). Then $N_e(\phi)$ shows the sinusoidal form of the anisotropic decay factor in $N_e(t)$ with an added phase shift that is proportional to the difference between reference oscillator and precession frequencies, $\Delta\omega$. The transformation from $N_e(t)$ to $N_e(\phi)$ has been done previously,[7] substituting $\phi=\omega_0 t$ in $N_e(t)$ and summing over all cycles of the reference oscillator from zero to infinity.

$$N_e(\phi)=e^{-\phi/\omega_0 t}\left[1+\frac{a}{R}\cos\left(\frac{\omega_H}{\omega_0}\phi-\theta-\alpha_0\right)\right],$$

where $\tan\alpha_0\cong(\omega_0-\omega_H)\tau$ and $R^2\cong 1+(\Delta\omega)^2\tau^2$.

The electrons are accepted during a 5.7 μsec gate after the muon stopping. A further refinement in method can be made by subdividing this gate at time T_1 and recording the $N_e(\phi)$ separately for each group; those electrons occurring from 0 to T_1 are designated early electrons, those from T_1 to 5.7 μsec are late electrons. As shown below, there is a phase shift between the early and late groups that is a sensitive function of the frequency difference between the muon spin precession and the reference oscillator.

$$N_e(\phi)^E=(1-e^{-T_1/\tau})\left[1+\frac{a}{RR_{T_1}}\cos\left(\frac{\omega_H}{\omega_0}\phi-\alpha_E\right)\right]e^{-\phi/\omega_0\tau},$$

$$N_e(\phi)^L=(e^{-T_1/\tau}-e^{-(T_1+T_2)/\tau})\times\left[1+\frac{a}{RR_{T_2}}\cos\left(\frac{\omega_H}{\omega_0}\phi-\alpha_L\right)\right]e^{-\phi/\omega_0\tau},$$

where T_1 is the length of the early gate, and T_2 the length of the late gate. $T_1+T_2=5.7$ μsec.

The phase shift between the two groups is

$$\alpha=\alpha_E-\alpha_L=(\omega_H-\omega_0)T_1-\alpha_{T_2}+\alpha_{T_1}.$$

The largest term is $(\omega_H-\omega_0)T_1$, which is the phase shift between the reference oscillator and the muon spin precession frequency after a time T_1. The α_{T_1} and α_{T_2} are small and nearly cancel, and additionally are nearly linear in $(\omega_H-\omega_0)$. They are a consequence of the finite lengths of T_1 and T_2, as are the amplitude modifying factors R_{T_1} and R_{T_2} (see Ref. 9).

The technique used for measuring ω_H, the muon spin frequency, is to vary the magnetic field, hence ω_H, about the value of ω_0. The values of α_E and α_L are determined at each field setting by Fourier analysis of the $N_e(\phi)$ and $\Delta\alpha$ is plotted as a function of field. $\Delta\alpha$ versus H is a near straight line with intercept ($\Delta\alpha=0$) when $\omega_H=\omega_0$.

The magnetic field is measured in terms of proton magnetic moments by nuclear magnetic resonance techniques, yielding f_p, and the ratio f_μ/f_p is the muon magnetic moment in proton moments.

III. DESCRIPTION OF THE SYSTEM

The method used here is basically the same as our previous measurement,[9] with the following improvements:

(1) The muons were stopped in a higher magnetic field so that their precession frequency was increased from 86 to 177 Mc/sec. The electronics was modified accordingly to operate at the higher frequency. This increased the precision by the above frequency ratio as the absolute frequency error, the other factors remaining equal, is fixed by the muon lifetme.

(2) The electron phase measurement was delayed until completion of the muon phase measurement so that there would be no error introduced by interference between the two analyzing circuits.

(3) More accurate calibration of the system was obtained by a more sophisticated muon precession simulator which made it possible to evaluate the effect of the muon lifetime on the calibration. This will be discussed more thoroughly below.

(4) The time resolution of the counter pulse was improved by using a tunnel diode and transistor zero crossing detector.

(5) The equipment was completely rebuilt with transistors for increased reliability.

(6) The reference oscillator frequency was decreased to the fourth subharmonic of the muon precession frequency. This avoided difficulties in designing high-frequency pulsed oscillators as will be discussed below.

(7) The intensity and quality of the muon beam at Nevis has been increased so that it was possible to achieve a statistical accuracy of 10 parts per million (ppm) in only 12 h running time. The data reported here were gathered in two cyclotron runs, Run II occurring a

year later than Run I. In Run II, there were the following additional changes.

(8) The muon and electron gates were replaced by a highly linear design to reduce error due to interference between gate pulse and timing pulses.

(9) A common paramagnetic fluid, water with $MnCl_2$ added, was used in the proton resonance probe and the target for muon resonance, so the paramagnetic shift to both f_μ and f_p would be the same and the ratio f_μ/f_p would be unaffected. This obviated the need for probe calibration.

A. Targets and Counters

A momentum selected beam of pions and muons enters the large magnet shown in Fig. 1. As it enters the field, it passes through $\frac{1}{2}$ in. of copper moderator designed to stop the muons in the target and the pions in the moderator, then passes through counters F_1 and 2. The beam turns approximately 90° in this field before reaching the center of the magnet where it is stopped in a target of 2-in. height, 3-in. width (perpendicular to the beam) and 1-in. thickness (in the beam direction). Any particles passing through the target will then penetrate counter 3.

Counters 2 and 3 are $\frac{1}{8}$-in.-thick plastic scintillators, shaped to just shadow the target, 2 in. by 3 in. Counters F_1 and F_2 are used for timing of the muon and electron pulses, respectively. They have 1-in.-thick plastic scintillators of $3\frac{1}{2}$-in. by $3\frac{1}{2}$-in. area. All counters have 2-ft Lucite light pipes to keep the photomultipliers out of the high field, and two layers of magnetic shielding were wrapped around the photomultipliers. RCA 7746 and Phillips 56-AVP photomultiplier tubes were used in counters F_1 and F_2 and RCA 6810, RCA 6655, and Phillips 56-AVP were used in counters 2 and 3 at different times during the experiment.

The target was supported in position by a 1-in.-wide Styrofoam platform which was attached to a brass framework clamped to the magnet. Styrofoam was used in the immediate vicinity of the target to minimize accidental events from muons stopping in this target support assembly. The target positioning was accomplished by pushing it along the platform until it reached a detent, then aligning the sides until they were even with the platform edges. The position could be reproduced to better than $\frac{1}{16}$ in. The target support assembly also held a nuclear magnetic resonance probe about 1 in. from the end of the target which monitored the field continuously.

B. Magnet

The magnet, Fig. 1, produced a field of 13.4 kG for this experiment. The large area of the pole faces, which were trapezoidal in shape with a base of 40 in., height of 24 in. and upper width of 18 in., permitted a comfortably large gap between the faces, $5\frac{1}{2}$ in., yet still retained good field homogeneity because of the high area to gap ratio. Nevertheless, considerable magnet shimming had to be done to obtain the required homogeneity over the target volume.

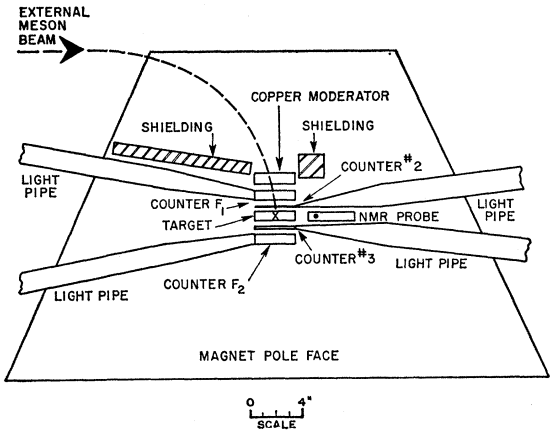

FIG. 1. Target and counter arrangement in the magnet.

In the initial shimming, shim steel was placed in the magnet yoke to tilt the pole faces relative to each other to remove gradients in the field. Further shimming was done by placing shim steel on the pole faces. These were placed on the underside of 1-in. magnet pole tips so that the effect of the shims would be spread over a greater volume in the target region and not tend to produce sharp peaks or dips in field strength.

To prevent damage or shifting of these shims during their removal and replacement in the shimming process, they were contained in a sandwich of two pieces of $\frac{1}{16}$-in. aluminum cut in trapezoidal pattern to fit the pole tip.

The final shimming was done with 0.001 in. shims on the gap side of the pole tips. These shims were also held in place by a $\frac{1}{16}$-in. aluminum plate to which they were taped. The final field had a rms deviation from its average value of 6 ppm over the target volume.

The magnet was supplied with a current of 150 A by a motor generator set. The total magnet current was regulated to 10 ppm by a transistor current regulator.[11] The voltage across a current shunt was put in series with a reference voltage of opposite polarity. The difference voltage was dc amplified by 10^8, and controlled the voltage drop across 30 paralleled power transistors through which the magnet current passed. During the data taking, the magnetic field was held constant by detecting the phase of a proton resonance signal from the monitor probe and putting this detector output signal in series with the reference voltage and the shunt voltage. Thus, when the field changed at the monitor probe position, the proton resonance signal phase changed and a voltage was produced by the detector which restored the field to its initial value. Field variations during the data taking were less than 10 ppm maximum and averaged less than 2 ppm.

[11] A. M. Patlach, IBM Research Report RW-19, 1960 (unpublished).

C. Electronics

1. Analyzing Logic

There are two further modifications to the method of measurement of muon-electron phase difference arising from the high frequency, 177 Mc/sec, of the muon spin precession. To avoid the difficulty of making phase measurements directly upon a high-frequency wave, the muon and electron counters start oscillators of frequency 5 Mc/sec from the reference oscillator. The outputs of the pulsed oscillator and the reference oscillator are mixed and detected, and the phase measurement is made upon the 5-Mc/sec "beat" frequency. At the time of the counter pulse, the phase of the "beat" is the same as the phase of the reference oscillator, except for a constant due to starting delay in the pulsed oscillator. This technique is equivalent to expanding the time scale.[12,13]

Also, the actual frequency of the reference oscillator was 44.4 Mc/sec, a factor of 4 less than the muon precession frequency. The necessary multiplication of this frequency to obtain equality with the muon spin frequency was obtained by the method used to store the data and is discussed below.

The block diagram of the system is shown in Fig. 2. Circuit diagrams may be found in a report by Hutchinson (see Ref. 25). A muon stopping in the target is indicated by a $F_1 2 \bar{3} \bar{F}_2$ coincidence. The output of the coincidence circuit goes to a gating circuit which generates a 5.7-μsec pulse, the muon gate. The 5.7-μsec time is determined by a delay line for stability. This gate releases a clamp on the muon pulsed oscillator. The muon timing pulse from counter F_1 passes through a tunnel diode pulse shaper for better time resolution and starts the muon oscillator which generates a prompt pulse and a 49.4-Mc/sec sine wave of 0.8-μsec length. The prompt pulse, called the start pulse, is delayed, then starts a voltage ramp by charging a capacitor with a constant current. The muon pulsed oscillator output, which is 5 Mc/sec higher than the reference oscillator, is mixed with the reference signal and the difference frequency is detected, shaped to a square wave and differentiated. This produces pulses when the beat crosses zero and one of these is gated by the delayed start pulse and stops the ramp. The ramp height is now proportional, except for an arbitrary constant, to the phase of the reference oscillator when the muon stopped in the target and started its precession.

Self gating of the zero crossing pulse, or stop pulse, is done to avoid distortion of this timing pulse by having it fall on the rising or falling edge of a gating pulse. The start pulse is delayed to allow starting transients in the pulsed oscillator to decay, then it opens a gate which lets through a stop pulse. This first stop pulse may be distorted by falling on a gate edge, but it triggers a 0.3 μsec gate which gates the next stop pulse, 0.2 μsec later. This second stop pulse is the one used to stop the ramp.

The 5.7-μsec muon gate also opens a gate through which a coincidence pulse indicating the decay electron, $\bar{F}_1 \bar{2} 3 F_2$, must pass. During the first run the electron analysis was delayed 1 μsec to minimize interference with the muon. In the second run due to improved circuitry this delay was not found necessary. The logic of the electron is similar to that of the muon; the electron coincidence generates an 8-μsec pulse, the electron gate. This gates the electron pulsed oscillator, which is triggered by counter F_2. The electron start pulse restarts the ramp and opens the first gate for the electron stop pulse, which stops the ramp at its final height.

However, the electron pulsed oscillator is at 39.4 Mc/sec, lower in frequency than the reference oscillator, while the muon pulsed oscillator is higher. As a result of the pulsed oscillator frequencies being on different

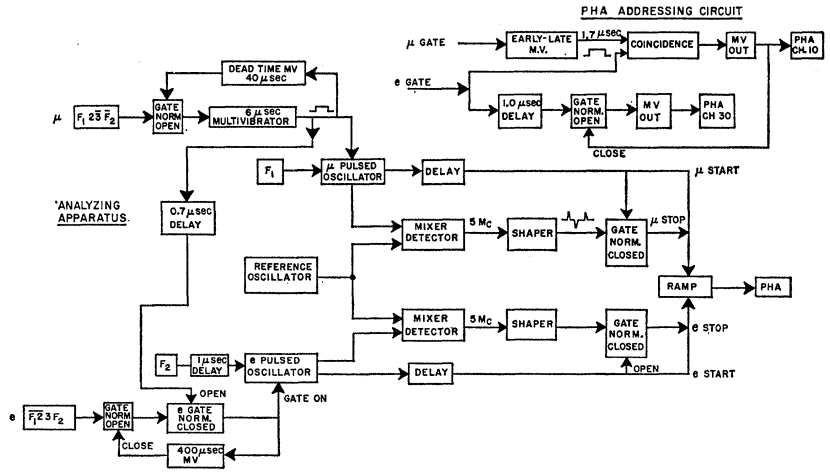

FIG. 2. Block diagrams of the phase analyzing circuit and the pulse-height addressing circuit.

[12] C. Cottini and E. Gatti, Nuovo Cimento 4, 1550 (1956).
[13] R. L. Chase and W. A. Higinbotham, Rev. Sci. Instr. 28, 448 (1957).

sides of the reference frequency, a phase measurement made with one beat note is negative with respect to that made with the other beat note, given the same starting phase of the pulsed oscillators relative to the reference oscillator. Thus, the sum of the two phase measurements represented by the ramp height is actually the difference between muon and electron phase. This voltage is stored in a commercial pulse-height analyzer (Penco Pa-4) by the read-out circuit.

The read-out circuit is triggered by the sum of muon and electron stop pulses so there is no read-out without both muon and electron, or when one of the pulsed oscillators is not triggered. Any time sensitive effect would introduce a spurious phase shift between the early and late electron distributions. Therefore, the read-out pulse is generated by a delayed muon stop pulse to minimize any difference in ramp voltage caused by the varying time delay of the electron relative to muon.

The internal logic of the pulse-height analyzer was modified for this experiment. The internal storage is controlled by two Burroughs tubes, each with one cathode and ten plates. One Burroughs tube controls the units, the other the tens. The tens tube was controlled externally in this experiment, but the units tube was unmodified.

External addressing was used to place all electrons of the early group in channels 10–19, all those of the late group in channels 30–39.

The muon gate triggered a monostable multivibrator, the early-late multivibrator, to produce a pulse of controlled length, T_1. The length of the multivibrator pulse, T_1, is the length of the early gate. The electron was put in coincidence with this pulse; a coincidence indicated an early electron, no coincidence, a late electron, and the appropriate tens channel in the pulse-height analyzer was addressed. Late electrons were those occurring at times from T_1–5.7 μsec after the muon.

The pulse spectrum folding of the pulse-height analyzer has two applications. For a given muon-electron phase difference, ϕ, two pulse heights may be produced, equivalent to ϕ and $\phi-2\pi$. ϕ ranges from -2π to $+2\pi$. The two output angles corresponding to the same phase ϕ are now addressed to the same pulse-height analyzer channel by adjusting amplifier gain so that the input pulse spectrum has a 20 channel range. This is folded into 10 channels as described above and the two phases ϕ and $\phi-2\pi$ fall into the same channel. The displayed set of ϕ now ranges from 0 to 2π.

As the frequency of the reference oscillator is $\frac{1}{4}$ the muon precession frequency, the displayed $N(\phi)$ would contain 4 wavelengths. To display just 1 wavelength, the amplifier gain is increased again by 4 times so the input pulse-height spectrum ranges over 80 channels. The folding is equivalent to the summing process that generated $N(\phi)$ from $N(t)$. In effect, it multiplies the reference frequency four times.

Changes in gain of the amplifier or frequency drifts in pulsed oscillator reduce the phase resolution of the system but do not produce any change in the measured ω_H. Loss of phase resolution reduces the apparent asymmetry, requiring more events to obtain the desired precision. The lower limit of phase resolution is fixed by the time resolution of the analyzing apparatus folded in with the time resolution of the scintillation counters. The resolution of the analyzing apparatus was 2 nsec, full width at half-maximum, which increased to 3 nsec when the equipment was used with scintillation counters.

The analyzing circuits were protected by controlled dead time circuitry, 40 μsec for a muon only, 400 μsec for muon and electron.

2. Test and Calibration Logic

(*a*) *Muon precession simulator.* In order to test the precision of the analyzing apparatus, it was necessary to devise elaborate test equipment. The muon precession simulator generates pulses with the same time distribution, except for the exponential lifetime factor, as a muon stopping and precessing in a magnetic field. The output from this circuit was used to trigger the pulsed oscillators and analysis proceeded as it would for real data. As the simulated precession frequency is known, the precession frequency calculated by the analysis system can be compared with it to detect any inherent error.

The logic of the muon precession simulator is shown in Fig. 3. The oscillator is adjusted to the desired precession frequency, near 177 Mc/sec, and its sinusoidal output added to a random source of pulses from a beta source illuminating a scintillation counter. The counter output pulse is clipped by 2 ft of shorted signal cable. The sum of the sine wave and the counter pulses enters a discriminator whose level is adjusted so that only the largest pulses trigger it. Consequently, the pulses selected by the discriminator are no longer random but are those occurring during the positive peak of the sine wave. The discriminator output triggers the appropriate gate. This phase selection is not sharp because of the pulse-height variations produced by the different beta energies. As this selection is done for both muon and electron, a phase correlation is produced between muon and electron channels. The early-late phase shift should

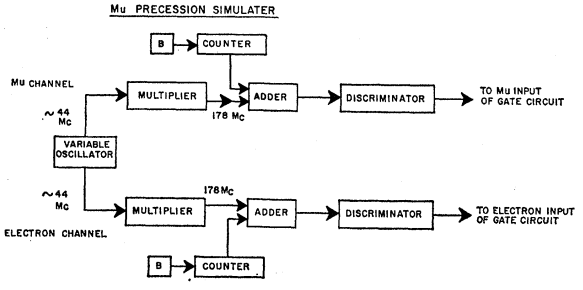

FIG. 3. Logic of muon precession simulator.

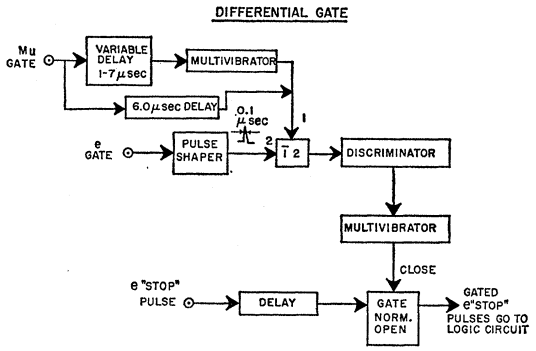

FIG. 4. Logic of the differential gating to find $\alpha(t)$.

be zero when the precession simulator is operating at the same frequency as the reference oscillator.

For most of the testing, the oscillator used to simulate the muon precession frequency was the reference oscillator with its frequency multiplied four times. The simulated muon and reference frequencies are then exactly equal and the $\Delta\alpha$ should be zero; the measured $\Delta\alpha$ is systematic error in the system. An independent oscillator was used for several tests to assure that error was not going undetected due to the phase correlation of both muon and electron with the reference oscillator.

(*b*) *Differential gate.* In order to find the effect of the muon lifetime on the $\Delta\alpha$, a gating was arranged so that α could be found as a function of time. Then it is possible to calculate the inherent $\Delta\alpha$, for any value of T_1, with the effect of the exponential decay of the muon taken into account, as will be discussed later. This was achieved by the use of two electron gates; a short one of 0.3 μsec duration, with variable delay relative to the muon and a fixed gate that accepted electrons in the time from 6.0 to 6.7 μsec after the muon. Note that electrons range from 1.0 to 6.7 μsec after the muon because of the 1-μsec delay in the electron channel. The delay of the short gate is variable from 1.0 to 5.0 μsec. If the early-late time, T_1, is set at 5.5 μsec between the two gates, then electrons falling in the short gate will be put in the early group and those in the 6.0–6.7 μsec interval in the late group. The $\Delta\alpha$ determined by Fourier analysis will be the phase shift of the electrons in the 0.3 μsec gate relative to those in the last 0.7 μsec of the electron gate. Thus, by varying the position of this short gate, α is found as a function of time with reference to the average α of electrons in the 6.0–6.7 μsec interval.

The logic of the differential gating (Fig. 4) is designed to avoid distortion of the timing pulses by the gating pulse. Similar logic was used for the linear gates used in Run II. The leading edge of the muon gate triggers a monostable multivibrator. This multivibrator produces a pulse of variable duration. The trailing edge of this pulse triggers a second multivibrator of 0.3-μsec pulse length, providing a gate of variable delay. This, plus the muon gate with 6.0-μsec delay, are put in anticoincidence with the leading edge of the electron gate. The output of the anticoincidence-coincidence triggers a third multivibrator which generates a 10-μsec pulse that saturates a transistor so that its collector shorts the electron start pulse, rejecting the event. These ungated events are the ones where the gating pulse is applied to the timing pulse. In the gated events there is no output from the coincidence circuit so the timing pulse is separated from the gating pulse by three stages of transistors, two of them biased off.

This logic has the disadvantage that it is not fail-safe; if the coincidence circuit fails to trigger the multivibrator or the multivibrator runs short, ungated events may be accepted. Discriminators and integrators were incorporated in the last three stages to minimize this possibility. To check this, the muon gate input was detached. No events were accepted during a 2-min test run, indicating feed through of less than 10^{-3}.

IV. EXPERIMENTAL PROCEDURE

The instrument magnet was located in its final position in the Nevis 50-MeV muon beam. No further movement of this magnet was made to avoid changing the field by the stress of lifting it. The magnetic field was mapped throughout the target volume. The proton resonance probe[14] used for mapping was attached to a three-dimensional translator so that all points could be reproduced.

A vibrating proton target[15] within the cyclotron has been developed at Nevis. This produces an external beam with a duty factor of 3, reducing the number of accidental events falling into the muon gate and decreasing loss of events due to dead time in the apparatus. The effective muon stopping rate in the target was about 1000/sec for an 8 gm, 2-in. by 3-in. target. Electron telescope solid angle was about 9%. The precession frequency of positive muons was measured in the following target substances:

Run I

methylene di-iodide, CH_2I_2
water
hydrochloric acid in water (37% HCl by weight)
bromoform, $CHBr_3$
copper
graphite

Run II

water+$MnCl_2$	carbon disulfide
lead	lithium
copper	sodium
calcium	potassium

The water and HCl targets were used for precision measurement of the muon moment. The other targets were used briefly to measure solid-state effects, shifts in

[14] "Numar" Yellow Probe No. 154A, Manufactured by Nuclear Magnetics Corporation, Boston, Massachusetts.
[15] J. Rosen, Nevis Report No. 92 (unpublished), Columbia University, New York, New York.

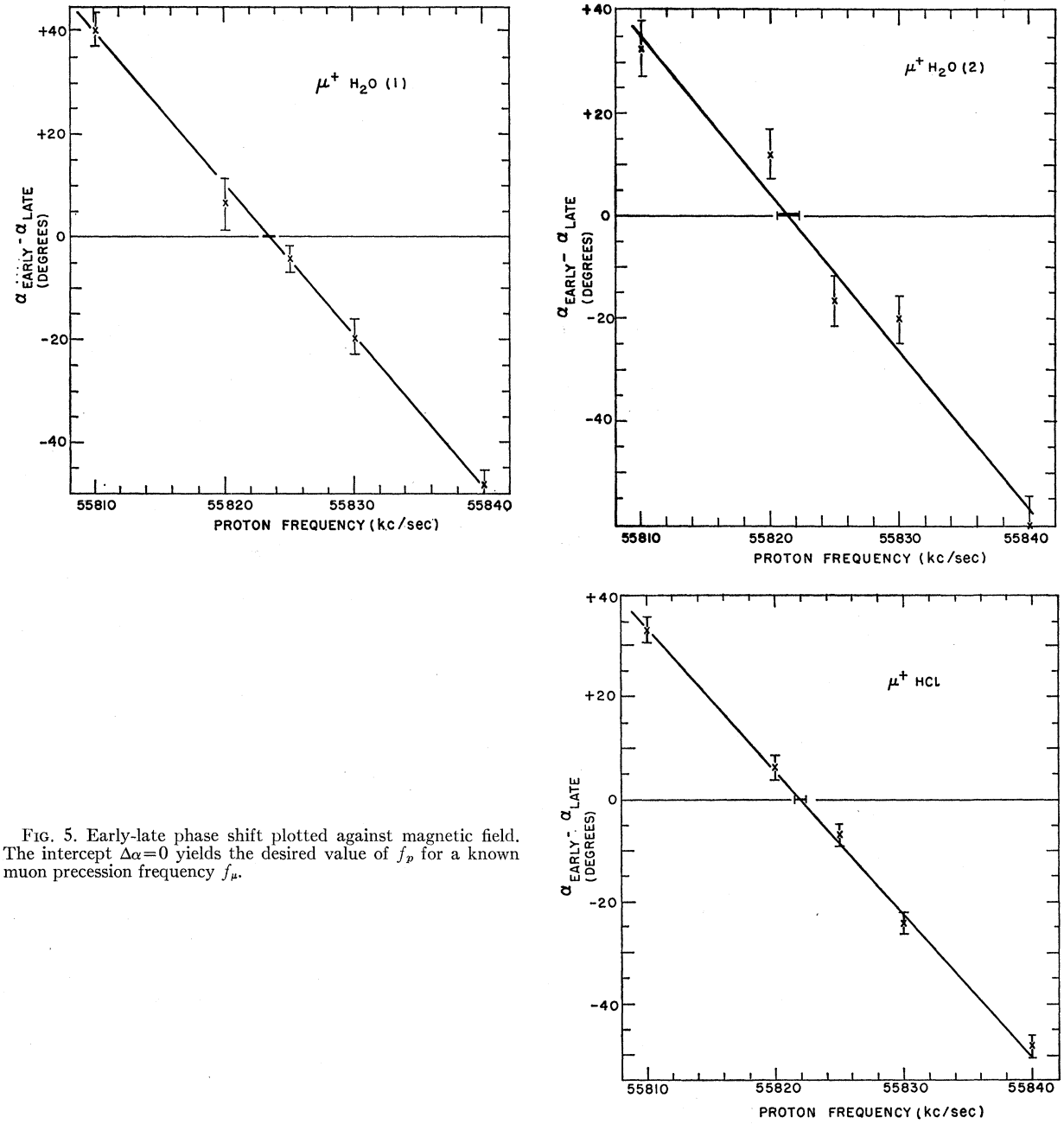

FIG. 5. Early-late phase shift plotted against magnetic field. The intercept $\Delta\alpha=0$ yields the desired value of f_p for a known muon precession frequency f_μ.

the muon frequency due to the magnetic field produced by the target substance at the muon stopping point. Also, negative muons were stopped in various materials. This article will discuss positive muons only; the following article will discuss the results obtained with negative muons. The apparatus was calibrated during the runs with the muon precession simulator.

V. ANALYSIS OF THE DATA

By Fourier analysis of $\mathrm{Ne}(\phi)$, the phase shift $\Delta\alpha$ is determined as a function of magnetic field (f_p) for each of the targets. Figure 5 shows a typical plot, with the desired proton frequency given by the horizontal intercept on this graph. The muon frequency is then equal to the reference oscillator frequency. Prior to tabulating these proton frequencies for each target, several systematic errors must be evaluated and corrected.

A. Corrections and Errors

1. Calibration of the Apparatus

To make an accurate measurement of the phase shift between the early and late groups of electrons requires

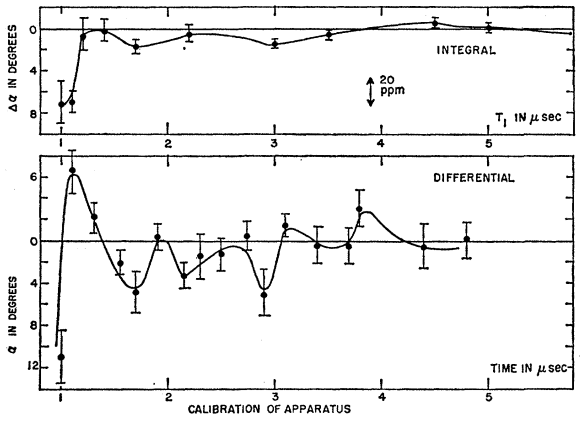

FIG. 6. Calibration curve of the apparatus. The upper curve is $\Delta\alpha$ for different early-late times, T_1. The lower curve is α as a function of time.

that there be no interaction between the muon and electron sections of the apparatus. Any effect on the electron channel due to the muon will probably be a function of time, hence, have a different effect on the early and late groups of electrons, producing a spurious phase shift. It is difficult to obtain the desired high degree of isolation because the muon and electron channels must be coupled at the gate circuit, where the muon gates the electrons for 5.7 μsec, and at the time-to-height converter (logic) where the muon and electron phase shifts are subtracted.

By operating the muon precession simulator at the same frequency as the reference oscillator, this inherent phase shift may be measured, as shown in Fig. 6. The calibration from Run I is used for illustration. The upper curve is $\Delta\alpha$ as a function of the time T_1, which divides the early and late groups. The lower curve is the $\alpha(t)$ of the electrons in a 300-nsec interval at time t relative to the muon, where $\alpha=0$ is taken as the average α in the 6.0–6.7 μsec interval.

As a consistency check, the two curves may be compared as follows:

$$\Delta\alpha(T_1)=\alpha_E-\alpha_L=\int_{1\ \mu\text{sec}}^{T_1}\alpha(t)dt\Big/(T_1-1)-\int_{T_1}^{6.7\ \mu\text{sec}}\alpha(t)dt\Big/(6.7-T_1).$$

The integration was performed numerically. A sample calculation with $T_1=2.3$ μsec gives $\Delta\alpha=-1.2°\pm1.0°$ calculated from the lower curve, compared with a $\Delta\alpha=-0.5°\pm0.8°$ shown on the upper curve. One degree equals 8 ppm. This is excellent agreement considering that the differential curve can be extended only to 5 μsec. The effect of the 5–6.7 μsec interval on α_L is unknown but is likely to be small as any disturbance induced by the muon will decrease with time. The agreement between the two curves can be seen qualitatively by the occurrence of positive and negative peaks in each at the same time.

The $\Delta\alpha$ for the actual experimental situation may now be calculated by putting the exponential time decay due to muon lifetime, τ, in the above equation:

$$\Delta\alpha(T_1)=\int_{1\ \mu\text{sec}}^{T_1}e^{-t/\tau}\alpha(t)dt\Big/(T_1-1)-\int_{T_1}^{6.7\ \mu\text{sec}}e^{-t/\tau}\alpha(t)dt\Big/(6.7-T_1),$$

$\tau=2.2$ μsec. $T_1=2.5$ μsec was used for this experiment so that there would be approximately equal numbers of electrons in the early and late groups. $\Delta\alpha$ for $T_1=2.5$ μsec is calculated to be $-0.6°$, or about 5 ppm. The accuracy of this calculation should be even better than the calculation above, as the exponential factor in the integrand makes the neglected 5–6.7-μsec interval $\alpha(t)$ relatively unimportant. Since the slope of $\Delta\alpha$ versus f_p is negative (Fig. 5), the correction, 5 ppm, must be added to the value of f_p determined by the intercept in Fig. 5.

Reference to the curve of $\alpha=\alpha(t)$ shows the very high error, on the order of 100 ppm, occurring for electrons in the first few tenths of a microsecond. However, the upper curve indicates that the positive and negative peaks cancel within 0.3 μsec. The upper curve is reliable here as the time is short relative to the muon lifetime, and a constant weighting is a good approximation.

In Run I, repeated measurements with the H_2O and CH_2I_2 targets suggested a possible downward drift in the apparatus, but the muon precession simulator did not show such a drift.

In Run II, a more extensive investigation was made of the calibration of the apparatus. The frequencies of the muon and electron oscillators were interchanged, changing the sign of the measured phase angle of the "beat" frequency. Thus, the sign of the slope of the plot of $\Delta\alpha$ versus f_p changes. The muon precession simulator indicated corrections of $+20$ and -10 ppm to the values of f_p determined with the pulsed oscillators in reversed and unreversed positions. If the same target is run with the oscillators in one position, then the other, the two measured values of f_p should differ by 30 ppm. However, when this was done with a magnesium target, the two f_p's differed by only 3 ± 10 ppm. This is a good indication that most of the shift is due to some error in the simulator itself. The indicated error in the apparatus is about 5 ppm as the corrections, -20 and $+10$ ppm, are of unequal magnitude. A 5 ppm error that was even (no sign change) under exchange of the oscillators plus 15 ppm odd error would yield the measured corrections. The odd error, 15 ppm, is not seen. The even error, presumably 5 ppm, is the most dangerous since it cannot be seen, by definition, with interchange of the oscillator. As the source of the errors is uncertain, no correction

is made for calibration, but an error of 5 ppm is allowed for the even part of the calibration correction.

Also in Run II, the possibility of systematic error due to recovery time in the electron counter was explored. The instantaneous singles rate in this counter was approximately 12 kc/sec. If there was a decrease in phototube gain following a pulse, then the early electrons would have a smaller average height than the lates, and a different delay due to puse height-time delay coupling in the electronics. To check this, the magnesium target was used again with the addition of an 18-μsec dead-time circuit triggered by single pulses from the electron counter. There was no change in the measured resonance frequency to within 7 ppm, the statistical accuracy. An error of 5 ppm is allowed for this effect.

2. Corrections due to Shifts in the Magnetic Field

The environment in which the muon stops changes the applied field. The muon enters into chemical combination with molecules of the target substance; the field at the muon receives a "chemical shift" due to the proximity of other nuclei and electrons. There is also a correction to the field due to bulk diamagnetism or paramagnetism of the target sample.

The "chemical shift" may be evaluated using data from proton magnetic resonance experiments. According to the Born-Oppenheimer approximation,[16] the positive muon should act chemically as a proton, as its mass is also much greater than that of the electron. As the muon lives only a few μsec, it is necessary to know the rate at which it forms compounds to know its final state. This is also estimated from data taken on protons.

Initially, the stopping muon comes to thermal equilibrium in the target substance, water, water plus HCl, or water plus $MnCl_2$, for the precision measurements. The muon will collide in about 10^{-13} sec with a neighboring water molecule. Because of the closeness of other water molecules, sufficient to carry away the 3–4 V binding energy, the probability for the formation of μH_2O^+ (analogus to hydronium) is very high, approaching one. The μH_2O^+ will transfer one of its protons or the muon to other water molecules in approximately 10^{-12} sec,[17] so the muon quickly reaches a final state of μHO, replacing one of the protons in a water molecule.

A very small fraction of the muons will be in μH_2O^+ form, approximately equal to the amount of H_3O^+ in pure water, $10^{-7}M$. In the aqueous HCl target the μH_2O^+ concentration is much higher, but still produces a change in magnetic field of only 4 ppm,[18] too small for us to see due to our statistical error, but still taken into account in our corrected result for f_μ/f_p.

Distilled water was used for the targets so there is no correction for bulk magnetic effects due to the presence of impurities. The magnetic field was measured by proton resonance, using protons in water. Therefore, there is no correction for the diamagnetic shielding of the protons or muons in water, as f_μ/f_p will not be changed. However, the probes had small amounts of paramagnetic impurities added to decrease their relaxation time so that they would be suitable for use with a 50 cycles per second (cps) field modulation nuclear magnetic resonance apparatus.

Therefore, they were calibrated against glycerine which had less than 5 ppm heavy metals. The gylcerine chemical shift is less than 1 ppm relative to water.[19] The monitor probe was found to be 8 ppm high and the mapping probe 10 ppm high. An error of 2 ppm is allowed for the presence of ferromagnetic impurities in the glycerine.

In Run II the problem of bulk shifts was avoided by using a common solution, water with a small amount of $MnCl_2$ added, for the field-measuring proton resonance probe and for the muon target.

In both runs a Lucite target container was used. About 25% of the muons stop in the Lucite, but, as the apparent asymmetry of Lucite is one third that of water, and the chemical shift expected of Lucite relative to water would range from 1–5 ppm,[20] the error due to chemical shift in the target container would be less than 1 ppm.

3. Magnetic Field

The magnetic field is not constant over the target volume, so the average field must be determined with account taken of the possibility of uneven distribution of the stopping muons over the target volume. The effect of time fluctuations in the field and of muons stopping outside the target volume must also be considered.

The largest error, after the calibration of the apparatus, is that due to muons stopping outside the target volume in the scintillators and Lucite light pipes of the counters. The magnetic field here is higher than the target average by 50–60 ppm. However, runs made with the target out yielded an apparent asymmetry of 0.024, roughly one-third that of water, and as only about one-fourth the total number of muons stopped outside the target, the weighted shift would be about 6 ppm. This correction, 6 ppm, is made to both Runs I and II and an error of 6 ppm is allowed.

The root-mean-square deviation of the magnetic field over the target volume was 6 ppm. The stopping muons were evenly distributed over the target vol-

[16] M. Born and J. R. Oppenheimer, Ann. Phys. (Paris) **84**, 457 (1927). Also see L. Pauling and E. B. Wilson, *Introduction to Quantum Mechanics* (McGraw-Hill Book Company, Inc., New York, 1935), p. 260.

[17] B. E. Conway, J. O'M. Bockris, and H. Linton, J. Chem. Phys. **24**, 834 (1956).

[18] J. A. Pople, W. G. Schneider, and H. J. Bernstein, *High Resolution Nuclear Magnetic Resonance* (McGraw-Hill Book Company, Inc., New York, 1959), p. 443.

[19] L. H. Meyer, A. Saika, and H. S. Gutowsky, J. Am. Chem. Soc. **75**, 4567 (1953).

[20] J. A. Pople, W. G. Schneider, and H. J. Bernstein, *High Resolution Nuclear Magnetic Resonance* (McGraw-Hill Book Company, Inc., New York, 1959), p. 272.

ume within 20%, so only 2 ppm error is assigned to field inhomogeneity.

The field fluctuates in time within 10 ppm limits. These fluctuations were observed by calibrated oscilloscope display of the proton resonance, and seemed to be symmetrical about the regulation point; 2 ppm is allowed for time fluctuations. The field is regulated directly by this proton resonance probe, the phase of the output signal from this probe is detected and used to control the magnet current. A correction must be made for the field difference between the average field over the target volume and the field at the probe position. There is an error in this measurement, 4 ppm, as determined by reproducibility.

B. Corrected Results

1. Solid-State Effects

Table I shows the muon asymmetry coefficients and frequency shifts relative to water for substances used.

The asymmetry coefficients are less than the expected value, 0.3, primarily due to the large solid angle subtended by the electron telescope at the target and the time resolution of the system. The error on these values is about 10%. They can be used on a relative basis, as conductors such as copper and magnesium do not depolarize. The asymmetry coefficient of copper is seen to be lower in Run II than in Run I due to a more compact geometry, hence larger solid angle for the electron telescope. Comparison within each run shows that CH_2I_2, $CHBr_3$ and the alkali metals do not depolarize stopping muons at this field, 13 kG. The slightly lower asymmetries for the liquids, CH_2I_2 and $CHBr_3$, are due to depolarization of muons stopping in their container.

TABLE I. Solid-state data.

	Target substance	Asymmetry coefficient	Frequency shift (ppm)	Frequency shift Knight shift (%)	Knight shift (ppm)
Run I	H_2O	0.09	...	...	...
	HCl	0.10	...	...	...
	CH_2I_2	0.15	− 25	...	...
	$CHBr_3$	0.14	− 14	...	...
	Copper	0.17	...	...	...
	Graphite	...	+380	...	...
Run II	Magnesium	0.12	+ 87	6.2	+1400[a]
	Copper	0.12	+ 81	3.5	+2320
	Lead	0.09	+132	11.0	+1200
	Calcium	0.09	+420	13.5	+3100[b]
	Water+$MnCl_2$	0.07	...	...	...
	Lithium	0.12	+ 11	4.4	+ 249
	Potassium	0.13	+ 88	3.1	+2900[b]
	Sodium	0.13	+ 79	7.0	+1130
	Carbon disulfide	0.04	...	...	...
	Lucite	0.05	...	...	...
	Target out	0.02	...	...	...

[a] T. J. Rowland, *Progress in Material Science* (Pergamon Press, Inc., New York, 1961), Vol. 9, p. 14.
[b] Predicted value.

Lead and calcium depolarize about 25%. Water depolarized about one third the stopping muons, in agreement with a previously reported measurement, at 50 G.[21] Lucite and carbon disulfide appear to depolarize as much as 80% of the stopping muons. The asymmetry values reported for these two substances may be somewhat higher than their true values as there would be a contribution from muons stopping outside the target; even a completely depolarizing target might produce an apparent asymmetry of 0.01. This has appreciable effect only for the highly depolarizing targets.

The second column of data in Table I is the frequency difference between muons in the target substance and muons in water. The error on these frequency shifts is about 10 ppm.

In Run I a negative shift (diamagnetic) is seen for CH_2I_2 and $CHBr_3$. The magnitude and sign suggest the formation of μI and μBr when muons are stopped in these targets,[22] the field shift being a chemical shift. A high paramagnetic shift was seen in graphite.

In Run II the muons were stopped in various conductors. The shift here would be due to conduction electrons at the muon stopping point increasing the local magnetic susceptibility. The bulk susceptibility of these samples was less than 20 ppm. Column IV shows the Knight shifts for these substances as tabulated by Knight.[23] Column III is our frequency shifts given as a fraction of the Knight shift.

The muon frequency shift is seen to be an order of magnitude smaller than the Knight shift. There is no reason to expect the muons to receive the full Knight shift, as this would require that all the muons stop at lattice points and that the enhancement of the conduction electron wave function be the same for the muon as for the nuclei at the other lattice points. A crude calculation based on the singlet annihilation rate of positrons stopped in metals—as this rate and the Knight shift are both proportional to the overlap of the positron (muon) and electron wave functions—indicates that a shift of 100 ppm would be expected. The large shifts in graphite and calcium are unexplained. Bulk paramagnetism due to impurities in the graphite can be ruled out, since measurements made on negative muons stopped in the same sample yielded the expected values.

2. The Magnetic Moment of the Free Muon

Summarizing the corrections and errors discussed above yields the muon magnetic moment:

[21] R. A. Swanson, Phys. Rev. **112**, 580 (1958).

[22] See the shifts of HI and HBr, relative to H_2O, J. A. Pople, W. G. Schneider, and H. J. Bernstein, *High Resolution Nuclear Magnetic Resonance* (McGraw-Hill Book Company, Inc., New York, 1959), p. 403.

[23] W. D. Knight, in *Solid State Physics*, edited by F. Seitz and D. Turnbull (Academic Press Inc., New York, 1956), Vol. 2, p. 122.

Run I corrections:

+0.34 kc/sec, muons outside target;
−0.43 kc/sec, probe calibration;
+0.28 kc/sec, apparatus calibration;
−4.90 kc/sec, monitor-target field difference.

A correction of 4 ppm, +0.22 kc/sec, is applied to the result of the HCl target for chemical shift. Then the corrected HCl frequency is averaged with the results of the water targets. The above corrections are applied to give $f_\mu/f_p=3.18340$.

The errors assigned are: 10 ppm, apparatus calibration; 6 ppm, muons outside target; 5 ppm, phototube recovery; 5 ppm, statistical; 2 ppm, probe calibration; 4 ppm, monitor-target field difference; 2 ppm, muon-stopping distribution in target; 2 ppm, time fluctuation in the magnetic field. Adding these in quadrature, the total error is 15 ppm.

$$f_\mu/f_p=3.18340\pm0.00005.$$

This moment measurement is 6 ppm different from that reported earlier for this run.[24,25] The difference arises from further evaluation of sources of systematic error as follows:

(1) The values for f_p in CH_2I_2 and $CHBr_3$ were used in the first report but were later discarded because of difficulty in evaluating the chemical shift in these substances.
(2) Recalibration of the apparatus, 3 ppm.
(3) The correction for muons stopping outside the target, 6 ppm.
(4) Allowance for recovery in the phototube, 7 ppm error.

Run II corrections: +0.34 kc/sec, muons outside target; −3.64 kc/sec, monitor-target field difference. Applying these corrections $f_\mu/f_p=3.18337$.

The errors assigned are: 7 ppm, statistics; 6 ppm, muons outside target; 5 ppm, calibration of apparatus; 5 ppm, phototube recovery; 4 ppm, monitor-target field difference; 2 ppm, muon-stopping distribution; 2 ppm, time fluctuation in the field. Again, adding in quadrature yields a total error of 13 ppm.

$$f_\mu/f_p=3.18337\pm0.00004.$$

Runs I and II are consistent with each other, differing by 10 ppm. For the final value of the muon moment we average the two values. We do not attempt to reduce the final error as three of the larger sources of error, the effect of muons stopping outside the target, apparatus calibration, and phototube recovery, might cause the same shift for both runs.

$$f_\mu/f_p=3.18338\pm0.00004 \quad (13 \text{ ppm}).$$

The above value of the muon magnetic moment is in agreement with our previous measurement,[9] 3.1834 ± 0.0002, to the extent that the larger error permits comparison, and is also in agreement with a recent measurement at the University of California, $f_\mu/f_p=3.18336\pm0.00007$.[26]

As discussed in the Introduction, this measurement of the muon magnetic moment may be used with the muon g factor reported by Charpak *et al.* and corresponding quantities for the electron to find to high precision the muon mass in terms of electron masses, assuming that $e_\mu=e_e$.

The most recent value[27] of f_e/f_p is 658.22759 ± 0.00004, the ratio of the spin-precession frequency of free electrons to that of protons in water. As the value of f_μ/f_p reported here is for both muon and proton bound in water, a correction must be made to one of the above values for the diamagnetic shielding of the bound muon or the proton. Making this correction,[28] 25.6 ppm, to the electron measurement yields $f_e/f_p=658.2107$. The g factor of the electron[29] is $2(1.0011609\pm0.0000024)$.

$$\frac{m_\mu}{m_e}=\frac{g_\mu}{g_e}\frac{(f_e/f_p)}{(f_\mu/f_p)}=206.765\pm0.003 \text{ (13 ppm)}.$$

This value is in good agreement with the aforementioned determinations of the muon mass by means of mesic x rays, $m_\mu/m_e=206.76\pm0.02$,[30–32] but represents a substantial increase in precision.

ACKNOWLEDGMENTS

The origination and early development of some of the techniques used in this experiment were largely the work of Professor R. L. Garwin and Professor S. Penman, to whom we express our indebtedness. We appreciate greatly the aid of Professor Allan M. Sachs, and Professor Leon M. Lederman who gave advice and encouragement during the course of this work. Professor Richard Bersohn and Professor Benjamin Dailey of the Columbia University Chemistry Department, and Pro-

[24] D. Hutchinson, J. Menes, G. Shapiro, A. Patlach, and S. Penman, Phys. Rev. Letters **7**, 129 (1961).
[25] D. Hutchinson, Nevis Report No. 103 (unpublished), Nevis Cyclotron Laboratories, Irvington-on-Hudson, New York.
[26] G. M. Bingham, Nuovo Cimento (to be published) and Lawrence Radiation Laboratory Report UCRL 10346, 1963 (unpublished).
[27] See J. W. DuMond, Ann. Phys. (N.Y.) **7**, 365 (1959).
[28] J. A. Pople, W. G. Schneider, H. J. Bernstein, *High Resolution Nuclear Magnetic Resonance* (McGraw-Hill Book Company, Inc., New York, 1959), pp. 170, 90, and 403.
[29] A. A. Shupp, R. W. Pidd, and H. R. Crane, Phys. Rev. **121**, 1 (1960).
[30] J. Lathrop, R. A. Lundy, V. L. Telegdi, R. Winston, and D. D. Yovanovich, Nuovo Cimento **17**, 109 (1960).
[31] J. Lathrop, R. A. Lundy, S. Penman, V. L. Telegdi, R. Winston, D. D. Yovanovich, and A. J. Bearden, Nuovo Cimento **17**, 114 (1960).
[32] S. Devons, G. Gidal, L. M. Lederman, and G. Shapiro, Phys. Rev. Letters **5**, 330 (1960).

fessor W. D. Knight of the University of California gave helpful information concerning the muon chemical environment in the targets. Many others of the Nevis staff gave generously of their time in our aid. Eugene Cianciulli, Warner Hayes, and Edmund Taylor helped in the construction and maintenance of our apparatus. Bob Eisenstein and Richard Isaacson participated in the early work on the experiment.

PHYSICAL REVIEW VOLUME 131, NUMBER 3 1 AUGUST 1963

Magnetic Moment of Negative Muons*

D. P. HUTCHINSON,† J. MENES,‡ AND G. SHAPIRO§
Columbia University, New York, New York

AND

A. M. PATLACH
IBM Watson Laboratory, New York, New York

(Received 3 January 1963)

The magnetic moment of negative muons bound in atoms of carbon, oxygen (in water), magnesium (metallic and in MgH_2), silicon, and sulfur has been measured with a precision ranging from 3×10^{-5} in carbon to 1.6×10^{-4} in sulfur. The measured moment is corrected for relativistic effects, diamagnetism, and nuclear polarization before being compared to the moment of the positive muon. The two moments are found to be equal to 3×10^{-4}, where the major uncertainty is due to Knight shift. The relativistic, diamagnetic, nuclear, and solid-state shifts are large enough compared to the statistical and systematic errors to make this technique usable for the investigation of these effects.

I. INTRODUCTION

THIS article, the second of two[1] dealing with muon magnetic moments, reports the extension of the technique for measuring these moments to negative muons bound in various atoms. Such a measurement is of interest for several reasons:

(a) A measurement of the negative muon magnetic moment and comparison with the positive muon would test the prediction, from *TCP* invariance, that the two muons, as particle and antiparticle, must have equal magnetic moments.

(b) Since the apparent magnetic moment is modified by the environment of the muon, the muon can be used as a probe. In particular, one might expect to observe nuclear effects, since the negative muon comes to rest in a Bohr orbit whose radius, because of the large muon mass, is comparable to nuclear radii for high Z.

With these two goals in view, measurements were made on muons stopped in graphite, water, magnesium, silicon, and sulfur. Graphite, where environmental effects were expected to be small, served to measure the moment. The experiments with the other materials were intended as investigations of environmental effects. All the targets used have zero-spin nuclei, to avoid depolarization through hyperfine interaction.[2]

Section II gives a brief description of those details in which this experiment differs from the one on positive muons, as described in Ref. 1. Section III contains the experimental results and a discussion of the environmental effects which modify the apparent magnetic moment.

II. EXPERIMENT

The experimental arrangement is described in detail in HMSP. The only difference is a shorter electron acceptance gate because of the shorter μ^- lifetimes.

The precision of the μ^- results is substantially less than that of the μ^+ results because of shorter lifetimes and lower asymmetry. It is worth reviewing certain features of the experimental technique to see exactly how the precision depends on lifetime and asymmetry.

As is explained in HMSP, the precession of the longitudinally polarized muon spin about a vertical magnetic field (of 13.4 kG), together with the asymmetric decay of the muon, produces a periodic variation, at the precession frequency, in the time distribution of decay electrons emitted in a fixed laboratory direction. This periodic variation (at 178 Mc/sec) takes the form of a sinusoid superimposed on the usual exponential decay. The experimental technique consists of comparing the frequency of this sinusoid with that

* This research is supported by the U. S. Office of Naval Research.

† Present address: University of Pennsylvania, Philadelphia, Pennsylvania.

‡ Present address: Brookhaven National Laboratory, Upton, Long Island, New York.

§ Present address: Lawrence Radiation Laboratory, University of California, Berkeley, California.

[1] The first article is: D. P. Hutchinson, J. Menes, G. Shapiro, and A. Patlach, preceding article, Phys. Rev. **131**, 1351 (1963); and will, henceforth, be denoted by HMSP.

[2] E. Lubkin, Phys. Rev. **119**, 815 (1960).